A structural basis for enhancement of long-term associative memory in single dendritic spines regulated by PKC

Jarin Hongpaisan*† and Daniel L. Alkon*‡§

*Blanchette Rockefeller Neurosciences Institute, Morgantown, WV 26506; †Laboratory of Neurobiology, National Institute of Neurological Disorders and Stroke, National Institutes of Health, Bethesda, MD 20892; and ‡Department of Neurology, West Virginia University Medical School, Morgantown, WV 26506

Communicated by Bernhard Witkop, National Institutes of Health, Bethesda, MD, October 5, 2007 (received for review June 1, 2007)

Using both scanning confocal and electron microscopic morphometric measurements, we analyzed single dendritic spines of CA1 pyramidal cells in the hippocampi of water maze-trained rats vs. controls. Two days after completion of all training, we observed a memory-specific increase in the number of mushroom spines—all of which make synaptic contacts—but not in the numbers of filopodia or stubby or thin spines, as quantified with double-blind protocols in both scanning confocal and electron microscopic images. This memory-specific increase of mushroom spine number was enhanced by the PKC activator and candidate Alzheimer's disease therapeutic bryostatin, blocked by the PKCα-isozyme blocker Ro 31-8220, and accompanied by increases in the number of "perforated" postsynaptic densities, increased numbers of presynaptic vesicles, and the increased occurrence of double-synapse presynaptic boutons associated with the mushroom spines. These and other confocally imaged immunohistochemical results described here involving PKC substrates indicate that individual mushroom spines provide structural storage sites for long-term associative memory and sites for memory-specific synaptogenesis that involve PKC-regulated changes of spine shape, as well as PKC-regulated changes of pre- and postsynaptic ultrastructure.

learning and memory | synaptogenesis | Alzheimer's disease | mushroom spines | bryostatin

As evidence has accumulated to support the hypothesis that synapses are critical storage sites for memory in the brain (1, 2), increasing attention has been given to dendritic spines (3). During development, dendritic spines appear to begin as thin extensions called filopodia that then mature with an expanded mushroom-shaped "head" linked by a neck to the dendrites (4). A recent two-photon laser analysis showed that single-spine enlargement is induced by long-term potentiation and glutamate release. This enlargement, however, only persists in small, nonmushroom spines (5, 6). Here, quantitative morphometric analyses in the CA1 dendritic areas were conducted with hippocampal slices taken from rats trained in the Morris water maze or exposed to control paradigms. Using double-blind protocols, a scanning confocal microscope was used to visualize different shapes of dendritic spines of CA1 apical dendrites by 1,1′-dioctadecyl-3,3,3′,3′-tetramethylindocarbocyanine perchlorate (DiI) staining. A second set of measurements, using double-blind protocols, involved electron microscopic visualization of pre- and postsynaptic ultrastructure associated with memory-specific changes of the mushroom spines. Confocal immunohistochemistry was also used to assess the total number of dendritic spines and presynaptic endings.

Results

A PKC-Activating Drug Enhances Learning and Memory. For water maze training of brown Norway rats (4–5 months old), there was an overall significant difference in learning among the experimental groups ($P < 0.001$; ANOVA). When treated with bryostatin, rats reached a hidden platform in a water maze more quickly than controls trained without bryostatin ($P < 0.001$; Fig. 1*a*). One day after rats had been previously trained in a Morris water maze for 6 days, memory retention was evaluated by the probe test. There were significant overall differences between experimental groups for the time taken by rats to reach the area of the underwater platform, now removed for probe testing ($P < 0.001$; Fig. 1*b*) and for the number of times that rats crossed the previous locations of the platform ($P < 0.001$; Fig. 1*c*). Bryostatin-treated maze-trained rats reached the previous area of the platform more quickly ($P < 0.05$) and crossed this location of the platform more times ($P < 0.02$) than maze rats injected with only the vehicle (Fig. 1 *b* and *c*). The bryostatin effects on learning ($P < 0.001$; Fig. 1*a*) and memory ($P < 0.01$ and 0.02; Fig. 1 *b* and c, respectively) were inhibited by the PKCα blocker Ro 31-8220. These results indicate that PKCα activation can enhance both learning and memory retention. It was previously shown that Ro 31-8220 inhibits rat brain PKCα *in vitro* with an IC_{50} at 5 nM, and Ro 31-8220 blocks the activity of PKCε, PKCβ_{I}, PKCβ_{II}, and PKCγ with an IC_{50} in the range of 14–27 nM (7). It should be noted, however, that the concentration used for Ro 31-8220 sufficient to block PKCα isozyme activity (but not other PKC isozymes) did not eliminate all maze learning and retention, suggesting that other PKC isozymes and/or other signaling molecules remained sufficiently functional to mediate learning and memory.

Memory and PKC Activation Increase Mushroom Spines. One day after the probe test (i.e., 2 days after completion of water maze training), DiI staining was first used for double-blind morphometric analyses of dendritic spines and synapses visualized with a confocal scanning microscope. Spines (vs. filopodia) have been defined as those postsynaptic structures that make a synaptic contact with at least one presynaptic ending (8). An ANOVA revealed a significant overall difference among the experimental groups for the mushroom spines ($P < 0.001$) and stubby spines ($P < 0.01$), but not for thin spines and filopodia (Fig. 1 *f–h*). Water maze training increased the numbers of mushroom spines ($P < 0.01$; Fig. 1 *e* and *f*) and the total spines (mushroom, stubby, and thin spines taken together; $P < 0.05$), but not the numbers of stubby or thin spines (Fig. 1 *g* and *h*) or filopodia. Administration of bryostatin during water maze training further enhanced the learning-induced increase in the number of mushroom spines ($P < 0.01$; Fig. 1 *e* and *f*), whereas Ro 31-8220 abolished it ($P < 0.001$; Fig. 1*f*). Bryostatin alone without training increased the number of stubby spines ($P < 0.001$; Fig.

Author contributions: J.H. and D.L.A. designed research; J.H. performed research; J.H. and D.L.A. analyzed data; and J.H. and D.L.A. wrote the paper.

The authors declare no conflict of interest.

§To whom correspondence should be sent at the * address. E-mail: dalkon@brni-jhu.org.

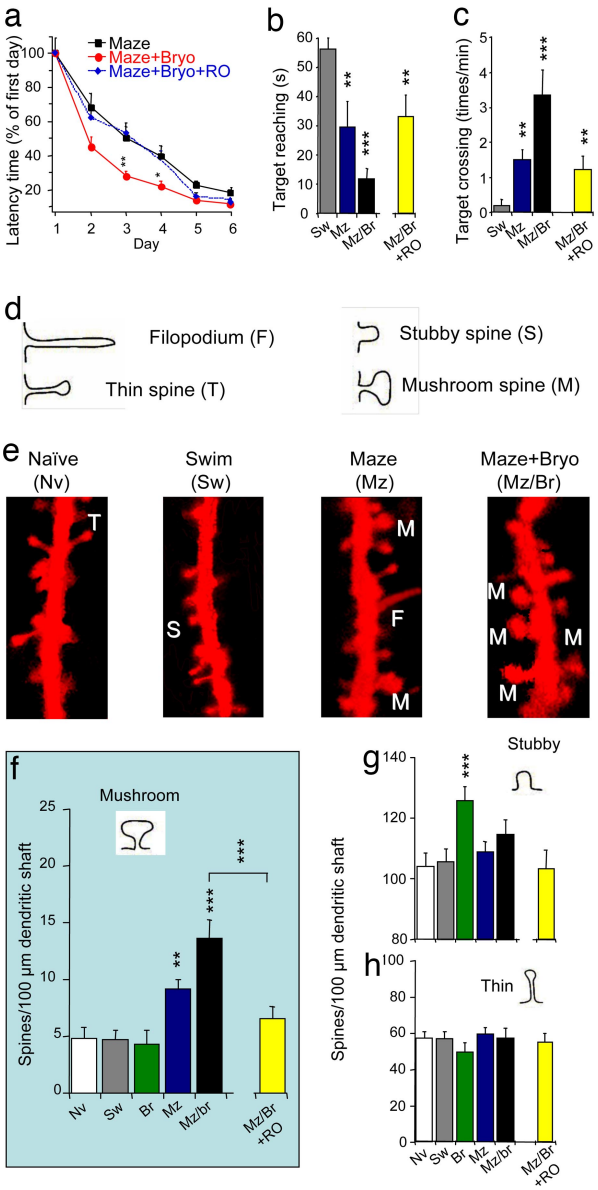

Fig. 1. DiI staining of dendritic spines. (*a*–*c*) Behavioral training. (*a*) Learning acquisition curves of rats trained over 6 days, four trials per day, in the Morris water maze. There was an overall significant difference in learning among the experimental groups ($F_{2,\ 427} = 6.815$, $P < 0.001$; ANOVA) for acquisition days 2–4. Administration of the PKC activator bryostatin n ($n = 11$ rats) increased the rate of learning indexed by reduced latencies ($F_{1,\ 315} = 10.772$, $P < 0.001$), whereas addition of the PKCα isozyme blocker Ro 31-8220 (RO; $n = 9$ rats) prevented the bryostatin enhancement ($F_{1,\ 271} = 11.307$, $P < 0.001$). (*b* and *c*) Memory retention 24 h after completion of training as evaluated by probe test measurements. There were significant overall differences between experimental groups for the time taken by rats to reach the area of the underwater platform, now removed for probe testing ($F_{3,\ 42} = 10.826$, $P < 0.001$), and the number of times that rats crossed the previous locations of the platform within 1 min ($F_{3,\ 42} = 9.070$, $P < 0.001$). Maze plus bryostatin rats ($n = 9$ rats) reached the platform area more quickly ($F_{1,\ 22} = 4.509$, $P < 0.05$) and crossed this location of the platform more times ($F_{1,\ 22} = 6.197$, $P < 0.02$) than did maze rats without bryostatin ($n = 12$ rats). These effects were inhibited ($n = 9$ rats) by Ro 31-8220 (*b*, $F_{1,\ 19} = 8.184$, $P < 0.01$; *c*, $F_{1,\ 19} = 6.181$, $P < 0.02$). (*d*–*h*) DiI staining and confocal microscopy at 24 h after probe test. Schematic drawings (*d*) and confocal images (*e*) show different shapes of dendritic spines and filopodia. There were significant overall differences among the experimental groups for the mushroom spines ($F_{5,\ 197} = 10.050$, $P < 0.001$) and stubby spines ($F_{5,\ 197} = 3.235$, $P < 0.01$), but not for thin spines and filopodia. (*f*) Water maze training ($n = 9$ rats, $n = 50$ dendrites) specifically increased mushroom spines in the stratum radiatum of hippocampal CA1 ($P < 0.01$; two-tailed *t* test) as compared with naïve ($n = 8$ rats, $n = 48$ dendrites) and swim ($n = 5$ rats, $n = 28$ dendrites) controls. Bryostatin (Mz/Br; $n = 6$ rats, $n = 29$ dendrites) further enhanced ($P < 0.01$) the learning-induced increase in the number of mushroom spines that was abolished ($P < 0.001$) by Ro 31-8220 ($n = 3$ rats, $n = 18$ dendrites). (*g*) Bryostatin alone ($n = 5$ rats, $n = 28$ dendrites) increased stubby spines ($P < 0.001$). (*h*) The number of thin spines was not affected by learning or PKC activation. Nv, naïve control; Sw, swim control; Br, bryostatin; Mz, water maze training. Asterisks over bars indicate significant differences as compared with both naïve and swim controls. Asterisks over brackets indicate significant differences between groups. *, $P < 0.05$; **, $P < 0.01$; ***, $P < 0.001$. ANOVA for behavioral experiments and two-tailed *t* tests were used for DiI staining.

1*g*) and thus total spine density ($P < 0.05$). Thus, learning increased mushroom spine formation. PKCα activation during learning further increased this mushroom spine formation, and PKCα activation alone only increased non-mushroom spines.

Immunohistochemistry Confirms the Memory-Induced Increase in the Total Number of Dendritic Spines. Changes of total dendritic spine numbers were further confirmed with confocal immunohistochemistry of the dendritic spine-specific protein spinophilin (Fig. 2*a*). At 2 days after the 6-day water maze training, quantification of the number of spinophilin granules showed a significant overall difference among experimental groups ($P < 0.001$). An increase in the total number of dendritic spines was apparent ($P < 0.05$; Fig. 2 *a* and *b*). Comparison between water maze training and water maze training with bryostatin demonstrated that bryostatin further enhanced the learning-induced increase in the number of dendritic spines ($P < 0.01$; Fig. 2*b*). The enhanced effect of bryostatin on dendritic spine density was attenuated by Ro 31-8220 ($P < 0.05$; Fig. 2*b*). In addition, bryostatin alone also increased the number of dendritic spines ($P < 0.01$; Fig. 2*b*).

Memory Does Not Increase the Number of Presynaptic Axon Boutons. In still other experiments (at the resolution of the confocal microscope), the presynaptic vesicle membrane protein synaptophysin was used as a marker for presynaptic axon boutons (Fig. 2*a*). No significant differences among the naïve control, swim control, water maze, and water maze plus bryostatin groups were observed for the number of synaptophysin-labeled endings ($P = 0.49$; Fig. 2*c*). This suggests that the number of the axon boutons was not affected by water maze training and/or bryostatin. Therefore, the increased number of mushroom spines induced by water maze training (and increased by bryostatin) might be hypothesized to form synapses with the existing axon boutons that already have synapses with other existing spines, resulting in an increase in the number of multiple-synapse boutons (9).

Memory Increases the Number of Presynaptic Vesicles. There was a significant overall difference among experimental groups for synaptophysin intensity ($P < 0.001$; Fig. 2 *a* and *d*) after water maze training. The fluorescence intensity of synaptophysin was increased in the water maze-trained animals as compared with naïve and swim controls ($P < 0.05$; Fig. 2 *a* and *d*), indicating increased numbers of presynaptic membrane vesicles that contain neurotransmitters. Water maze training plus bryostatin had even higher synaptophysin intensity than water maze training without bryostatin ($P < 0.05$; Fig. 2*d*), suggesting a PKC-mediated increase in presynaptic vesicle number. Ro 31-8220 did not, however, suppress the bryostatin-enhancement of the maze-induced increase in synaptophysin intensity (Fig. 2*d*), suggesting a dependence on other bryostatin-activated isozymes such as PKCε and/or PKCδ that were not blocked by the Ro 31-8220 used.

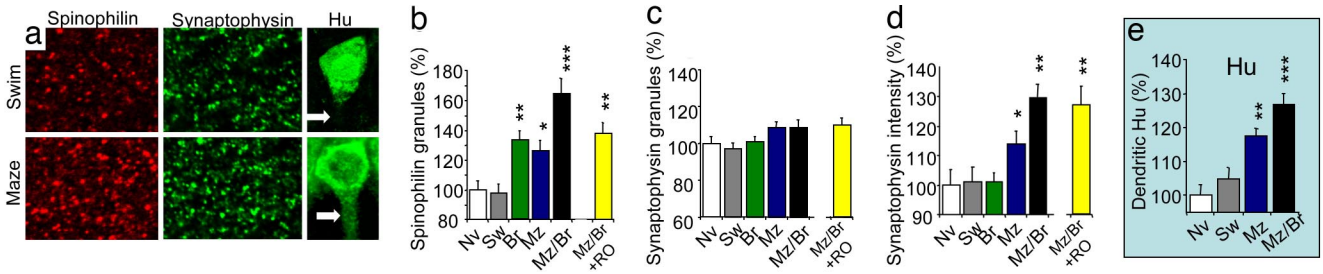

Fig. 2. Immunohistochemistry of pre- and postsynaptic compartments. (*a*) Scanning confocal microscopy of hippocampal CA1 areas: the dendritic spine marker spinophilin (*Left*) (each granule is one dendritic spine), the presynaptic axonal bouton marker synaptophysin (*Center*) (each granule is one axon bouton), and PKC-dependent Hu proteins (*Right*) (or mRNA-stabilizing proteins ELAV). Two days after 6-day water maze training, we observed sustained translocation of Hu proteins from the nucleus into the dendrite (arrow) together with an increase in the number of dendritic spines marked with spinophilin and increased synaptophysin intensity. (*b*) Quantification of the number of spinophilin granules showed a significant overall difference among experimental groups ($F_{4,\ 177} = 8.535$, $P < 0.001$; ANOVA). Water maze training ($n = 6$ rats; $n = 59$ CA1 images; $P < 0.05$; two-tailed *t* test) increased the numbers of dendritic spines as compared with naïve and swim controls ($n = 3$ rats; $n = 30$ images in each control). These effects were enhanced by bryostatin ($n = 4$ rats; $n = 32$ images; $P < 0.01$). The enhanced effect of bryostatin was suppressed by Ro 31-8220 ($n = 3$ rats; $n = 30$ images; $P < 0.05$). Bryostatin alone also increased the number of dendritic spines ($n = 3$ rats; $n = 30$ images; $P < 0.01$). (*c*) ANOVA showed no significant difference among the naïve control, swim control, water maze, and water maze plus bryostatin groups for the number of synaptophysin granules ($F_{4,\ 219} = 0.855$, $P = 0.49$). The results in *b* and *c* indicate that memory retention is associated with increased numbers of mushroom spines but no changes in the numbers of presynaptic axonal boutons. Therefore, *de novo* dendritic spines may form synapses with the existing axonal boutons, resulting in an increase in the number of multiple-synapse boutons, as described in ref. 9. (*d*) Quantification of synaptophysin intensity shows that there was a significant overall difference among experimental groups for synaptophysin intensity ($F_{4,\ 226} = 5.742$, $P < 0.001$). Water maze training increased synaptophysin intensity ($n = 6$ rats; $n = 60$ images; $P < 0.05$) as compared with naïve ($n = 3$ rats; $n = 30$ images) and swim ($n = 6$ rats; $n = 60$ images) controls. The effect of water maze training on synaptophysin intensity was enhanced by bryostatin ($n = 5$ rats; $n = 47$ images; $P < 0.05$). This suggests that memory also augments presynaptic vesicle numbers in multiple-synapse boutons to maintain the capacity to activate increased numbers of postsynaptic membranes (presumably with the mushroom spines). The bryostatin enhancement of water maze training-induced increase in the number of dendritic spines (*b*), but not presynaptic vesicle number (*d*), was attenuated by the PKCα blocker (RO). These results suggest that the effects of learning and bryostatin on the postsynaptic compartment are PKCα-dependent, whereas those effects on presynaptic compartment are not PKCα-dependent. (*e*) Quantification of dendritic Hu protein intensity (three to four rats in each experiment) showed that Hu proteins in CA1 dendrites showed a significant overall difference among experimental groups ($F_{3,\ 201} = 16.424$, $P < 0.001$). Two days after 6-day water maze training, water maze training increased the nuclear export of HuC and HuD proteins into the dendritic shaft ($n = 57$ dendrites; $P < 0.01$) as compared with naïve ($n = 64$ dendrites) and swim ($n = 45$ dendrites) controls. Bryostatin ($n = 36$ dendrites) further enhanced the learning-induced accumulation of Hu ($P < 0.05$; water maze training vs. water maze training with bryostatin). These results confirmed a previous report that water maze training increased PKCα-activated translocation of Hu proteins to dendrites (11). However, the present study also demonstrated that bryostatin promoted memory-induced Hu protein accumulation in dendrites. Asterisks indicate significant differences as compared with both naïve and swim control groups. *, $P < 0.05$; **, $P < 0.01$; ***, $P < 0.001$.

Sustained Activation of PKCα-Dependent, mRNA-Stabilizing Proteins ELAV After Water Maze Training. Learning was previously found to activate PKCα-dependent Hu proteins (or mRNA-stabilizing proteins ELAV) that promote protein synthesis by blocking mRNA degradation (10–12). Hu proteins and other mRNA-stabilizing proteins also were suggested to accumulate in dendritic shafts (10) and thus might be important for spine formation. Using confocal microscopy combined with immunohistochemistry, we found that Hu proteins in CA1 dendrites showed a significant overall difference among experimental groups ($P < 0.001$). The water maze training group increased the nuclear export of HuC and HuD proteins into the dendritic shaft followed by prolonged accumulation, even at 2 days after 6-day water maze training ($P < 0.01$; Fig. 2 *a* and *e*) (11). Bryostatin further enhanced the learning-induced accumulation of Hu ($P < 0.05$; Fig. 2*e*).

Electron Microscopy (EM) Confirms the Memory-Induced Increase in the Number of Mushroom Spines. Double-blind EM was then used to confirm changes in mushroom spines and their presynaptic axonal boutons as determined by the above confocal microscopy at 2 days after 6-day water maze training. These animals showed learning behavior similar to the average values of the larger animal groups in Fig. 1*a*. An ANOVA revealed a significant overall difference among the experimental groups for the number of mushroom spines ($P < 0.001$). These EM results (Fig. 3*c*) confirmed the results obtained with confocal DiI staining (Fig. 1*f*) and immunostaining (Fig. 2*b*) showing that water maze training significantly increased the number of mushroom spines ($P < 0.05$), and that the combination of bryostatin with water maze training further increased mushroom spine number ($P < 0.01$; Fig. 3*c*).

It should be noted that the number of mushroom spines represents only a small percentage (5–15%) of the total number of spines on the dendrites. Thus, the memory-specific and bryostatin-enhanced increase of mushroom spine number is affecting a restricted subclass of spines apparently important for memory retention.

Memory Increases the Numbers of Multiple-Synapse Boutons and Presynaptic Vesicles Revealed by EM. Quantitative analysis of the percentages of boutons with a high number of presynaptic vesicles (Fig. 4*a Right*) showed a significant overall difference among the experimental groups ($P < 0.001$; ANOVA). In confirmation of the confocally demonstrated increased intensity of synaptophysin (Fig. 2*d*), water maze training increased the number of presynaptic vesicles (as visualized with EM) in the axon boutons of mushroom spines ($P < 0.01$), an effect that was significantly enhanced by bryostatin ($P < 0.01$; Fig. 4*b*). In addition, the EM data also showed a significant overall difference ($P < 0.001$) in the number of axon boutons that formed multiple synapses with at least one mushroom spine and another (thin, stubby, or mushroom) spine(s) (Fig. 4*a Right*) and confirmed that the axonal boutons of mushroom spines in water maze rats were more likely to be multiple-synapse boutons ($P < 0.05$; Fig. 4*d*). This increased effect was also enhanced by bryostatin ($P < 0.01$; Fig. 4*d*).

Effects of Memory and PKC Activation on Mushroom Spines with Macular or Perforated Postsynaptic Density (PSD). Postsynaptic compartments of mushroom spines were further studied by electron

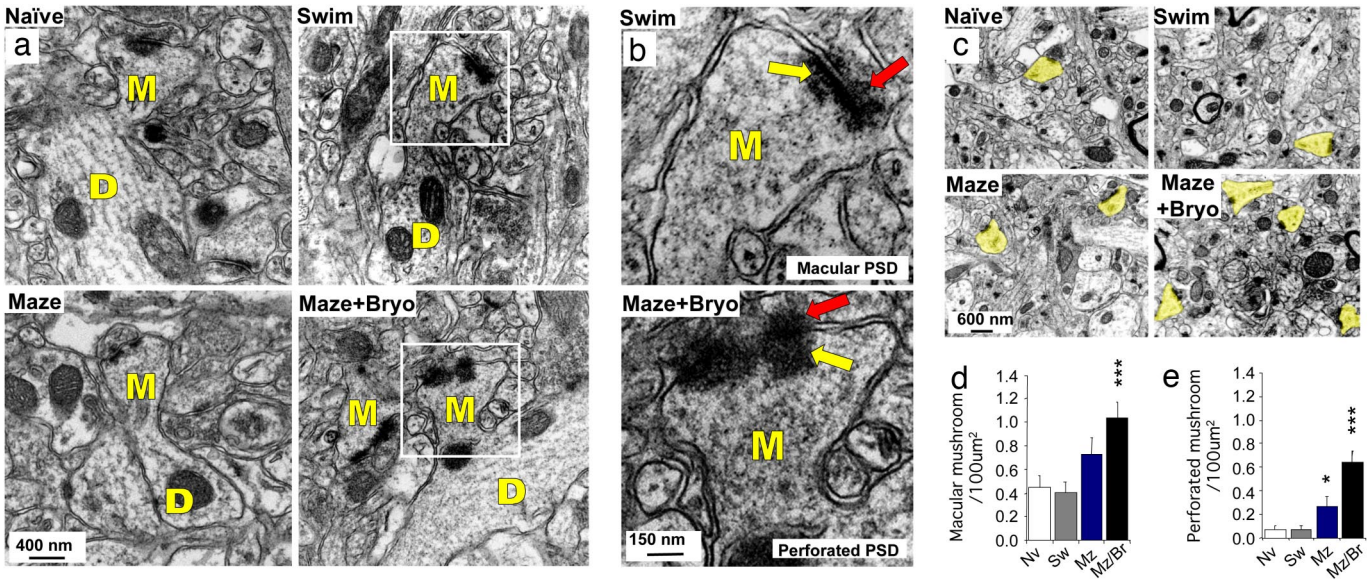

Fig. 3. EM of mushroom spines. (*a*) Double-blind analysis of electron micrographs shows the ultrastructure of mushroom spines in the CA1 hippocampal area at 2 days after 6-day water maze training ($n = 3$ animals in each condition). (*b*) Higher magnification (area indicated by boxes in *a*) shows the morphology of macular and perforated PSD (yellow arrows) and their presynaptic membrane (red arrows) partners. (*c*) Lower magnification showed changes in the numbers of total mushroom spines (highlighted in yellow). M, mushroom; D, dendrite. (*d* and *e*) Electron micrographs were analyzed for the numbers of macular (*d*) and perforated (*e*) PSD mushroom spines. There were significant overall differences among experimental groups for macular ($F_{3,\ 224} = 6.647$, $P < 0.001$) and perforated ($F_{3,\ 224} = 16.530$, $P < 0.001$) PSD mushroom spines. (*d*) For macular PSD, only water maze training with bryostatin showed a significant different ($P < 0.001$) from naïve and swim controls. (*e*) For perforated PSD, water maze training increased the number of perforated PSD-containing mushroom spines ($P < 0.05$) as compared with naïve and swim controls. This effect was enhanced by bryostatin ($P < 0.01$; water maze training vs. water maze training with bryostatin). Quantification of total mushroom spines (i.e., the numbers of macular and perforated spines taken together) showed a significant overall difference among experimental groups ($F_{3,\ 224} = 16.825$, $P < 0.001$). Water maze training ($n = 3$ animals for each condition) significantly increased ($n = 49$ micrographs; $P < 0.05$) the number of mushroom spines as compared with naïve ($n = 55$ micrographs) and swim ($n = 56$ micrographs) controls. These numbers were further enhanced by bryostatin ($n = 65$ micrographs; $P < 0.01$; water maze training vs. water maze training with bryostatin). Asterisks indicate significant differences as compared with both naïve and swim control groups. *, $P < 0.05$; ***, $P < 0.001$.

microscopic quantification of macular (continuous) and perforated (middle hollow) PSDs (Fig. 3*b*, yellow arrows). An ANOVA revealed significant overall differences among the experimental groups for the number of macular or perforated mushroom spines, and their presynaptic structures: presynaptic vesicles and multiple-synapse boutons ($P < 0.001$ in all comparisons). The effects of water maze training on the increased number of mushroom spines ($P < 0.05$; Fig. 3 *a*, *d*, and *e*) and

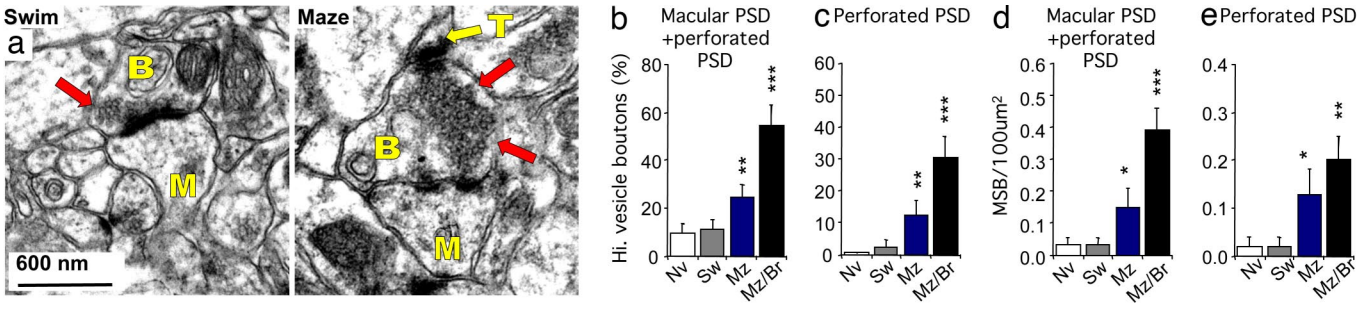

Fig. 4. EM of presynaptic axonal boutons of mushroom spines. (*a*) Ultrastructure of axon boutons (B) that synapse with mushroom spines (M) in hippocampal CA1 area at 2 days after 6-day water maze training. Note the increased number of presynaptic vesicles (red arrows) in presynaptic boutons and the presence of two spines (M, mushroom; T, thin) that synapse with the bouton for water maze-trained rats. (*b* and *c*) Quantification of presynaptic axon boutons with a high volume of presynaptic vesicles showed significant overall differences among experimental groups for axon boutons of total (macular and perforated PSD; $F_{3,\ 206} = 13.344$, $P < 0.001$), macular PSD ($F_{3,\ 206} = 2.526$, $P < 0.05$), and perforated PSD ($F_{3,\ 204} = 12.461$, $P < 0.001$) mushroom spines. Water maze training significantly increased the number of axon boutons with a high volume vesicles of perforated ($n = 49$ micrographs; $P < 0.01$), but not macular, mushroom spines as compared with naïve ($n = 55$ micrographs) and swim ($n = 57$ micrographs) controls. This results in a significant increase in presynaptic vesicles in the axon boutons of overall mushroom spines ($P < 0.01$). These effects were significantly enhanced by bryostatin ($n = 46$ micrographs; $P < 0.01$ for *b*; $P < 0.05$ for *c*; water maze training vs. water maze training with bryostatin). (*d* and *e*) Quantification of multiple-synapse boutons (MSB) showed significant overall differences among experimental groups for total ($F_{3,\ 238} = 12.566$, $P < 0.001$), macular PSD ($F_{3,\ 238} = 24.820$, $P < 0.001$), and perforated PSD ($F_{3,\ 238} = 5.818$, $P < 0.001$) mushroom spines. Water maze training significantly increased the number of multiple-synapse boutons of perforated ($n = 53$ micrographs; $P < 0.05$), but not macular, mushroom spines as compared with naïve ($n = 59$ micrographs) and swim ($n = 61$ micrographs) controls. This results in a significant increase in multiple-synapse boutons of total mushroom spines ($P < 0.05$). The effects of water maze training were significantly enhanced by bryostatin ($n = 66$ micrographs; $P < 0.01$ for *e*; water maze training vs. water maze training with bryostatin). Asterisks indicate significant differences as compared with both naïve and swim control groups. *, $P < 0.05$; **, $P < 0.01$; ***, $P < 0.001$.

changes of their presynaptic boutons—i.e., increases in presynaptic vesicles ($P < 0.01$; Fig. 4*c*) and multiple-synapse boutons ($P < 0.05$; Fig. 4*e*)—were all restricted to those mushroom spines that contained perforated PSDs.

When bryostatin was combined with water maze training, the increased numbers of perforated PSD-containing mushroom spines ($P < 0.001$; Fig. 3*e*), presynaptic vesicles ($P < 0.001$; Fig. 4*c*), and multiple-synapse boutons ($P < 0.01$; Fig. 4*e*) were more increased than for water maze training without bryostatin. In contrast to water maze training, bryostatin plus water maze training also increased the number of macular PSD mushroom spines ($P < 0.001$; Fig. 3*d*) that formed synapses with multiple-synapse boutons ($P < 0.001$) with high numbers of presynaptic vesicles ($P < 0.01$).

Enhancement of Protein Synthesis by the PKCα Activation of mRNA Stabilizing Proteins ELAV Increases the Number of Dendritic Spines. To further investigate the role of bryostatin on PKC-dependent ELAV or Hu proteins in spinogenesis, hippocampal slices (four to six slices from three to four rats in each experiment) were studied *in vitro*. Consistent with previous studies that demonstrated translocation to the plasma membrane and activation of PKC in CA1 neurons during behavioral training (14), exposure to sustained bryostatin (0.1 nM) application for 120 min (i.e., *in vitro*) caused increased translocation of HuC/D to the dendrites ($116 \pm 3\%$; $n = 65$ dendrites; $P < 0.01$) as compared with the control without-bryostatin incubation ($n = 118$ dendrites). Furthermore, the number of dendritic spines after *in vitro* bryostatin incubation was also significantly augmented [$201 \pm 20\%$ ($n = 24$ random CA1 images); $P < 0.01$ ($n = 18$ images)] as measured by spinophilin. This *in vitro* increase in spine number was inhibited by the PKCα blocker Ro 31-8220 at 10 nM [$76 \pm 5\%$ ($n = 37$ images); $P < 0.001$] and by the protein synthesis blocker cycloheximide (20 μM; Sigma–Aldrich) [$86 \pm 7\%$ ($n = 37$ images)]. These results suggest that bryostatin-induced increases in dendritic spine number depend on protein synthesis, perhaps because of increased local protein synthesis induced by the PKCα-activated, mRNA-stabilizing protein Hu in dendrites.

Discussion

The evidence for PKC-regulated structural changes in spines during memory retention is consistent with previous demonstrations of memory-specific, cytosol-to-membrane translocation of PKC in dendritic regions of the mammalian hippocampus (13, 14). Memory-specific enhancement of synaptic potentials in the CA1 pyramidal cells that were elicited by Schaffer collateral stimulation was also shown to be inducible by exogenous PKC activation (15). Furthermore, PKC signaling pathways regulate dendritic spine morphology in juvenile brain slices and in cultured neuronal synaptic preparations (16–18).

Training paradigms that produce associative memory such as trace eyeblink conditioning (9, 19) and fear conditioning (20) have previously been found to cause increases of dendritic spine density and/or multiple-synapse boutons. The results described here establish that it is the mushroom spines, together with their associated presynaptic partners, that occur in markedly increased numbers during memory retention, thus indicating memory-induced synaptogenesis. Long-term potentiation, however, did not cause persistent changes of mushroom spines (5, 6). The results described above also suggest that bryostatin's PKC-enhancing effect on spine number is redirected by the learning paradigm from the stubby to the mushroom spines. Memory induction and bryostatin, a candidate drug for the treatment of Alzheimer's disease (24), also promote an increased proportion of "perforated" and macular PSDs as well as increased numbers of presynaptic boutons that synapse with mushroom spines together with at least one additional spine. The *in vitro* immunohistochemistry further confirmed bryostatin's PKC enhancement of spine number as indexed by postsynaptic spinophilin. That these synapses were made more competent for transmitter release was suggested by the bryostatin-induced increases of synaptophysin fluorescence intensity and EM-visualized presynaptic vesicles. Finally, the *in vivo* bryostatin effects on the PKCα-substrate Hu protein movements into the proximal dendritic shafts suggests that this could be an important step in PKC-mediated control of memory-induced changes of synaptic spines and their presynaptic partners.

Materials and Methods

Spatial Maze Tasks. Brown Norway rats (4–5 months old; 280–330 g; from National Institutes on Aging, Bethesda) were trained on a water maze as described in refs. 11 and 21. At 60 min before water maze training on days 1, 3, and 5, tail-vein injection was used to administer Ro 31-8220 (Sigma–Aldrich; 500 μg/kg body weight) or vehicle. After 30 min, bryostatin (kindly provided by the National Cancer Institute, Bethesda) or vehicle was administered i.p. at 10 μg/kg body weight ($\cong$60 μg/m^2 body surface). Rats were trained with four trials per day for 6 consecutive days. The escape latency was measured on each training day and on days when a probe test was also conducted (i.e., 24 h after last training).

Confocal *in Vivo* Experiments. One day after a probe test, under anesthesia (choral hydrate; Sigma–Aldrich; 400 mg/kg body weight, i.p.), rats were perfused through the heart with PBS by gravity to wash out the blood and then lightly fixed with $\approx$150 ml of 4% paraformaldehyde in PBS at room temperature, instead of a cold fixative, because hypothermia can reduce the number of dendritic spines (22). Brains were removed and postfixed for 10 min. Thereafter, hippocampi were isolated from the right brain hemispheres, and dorsal hippocampi were sectioned with a vibratome at 400 μm for DiI staining and immunohistochemistry.

DiI Staining. The tips of glass electrodes, prepared as used for electrophysiology, were immersed in 5% (wt/vol) DiI (Molecular Probes/Invitrogen) in dichloromethane (Sigma–Aldrich) and air-dried at room temperature for 30 min. The tips of DiI-coated electrodes were inserted, broken, and left in the strata oriens of CA1 area of hippocampal sections at 400 μm thickness. After maintenance in PBS at 4°C overnight to allow DiI to diffuse in the plasma membrane of CA1 neurons, hippocampal sections were then resectioned to 35 μm thickness and mounted on glass slides, using PBS as the mounting medium. Dendritic spines stained with DiI in the strata radiatum were collected by using a Zeiss Axiovert 200M microscope equipped with 510 confocal scanning system at 568 nm/>510 nm (excitation/emission). A stack of confocal images (taken every 0.4 μm) was collected to obtain all dendritic spines of an individual dendritic shaft. During analysis, a stack of images was retrieved with the ImageJ program (http://rsb.info.nih.gov/ij). Individual spines identified on one image were also verified on adjacent stacked images to approximate the three-dimensional structure of this spine. Those spines, which had head diameters more than three times larger than the diameter of their necks (Fig. 1 *d* and *e*), were identified as mushroom spines. Approximately four to six stacked image sets were obtained from each animal. All image sets were pooled and coded; therefore, images were identified with unknown animal number and unknown treatment (double-blind protocol).

Immunohistochemistry. Hippcampal slices at 400 μm thickness were further immersed in the fixative (4% paraformaldehyde in PBS) for 30 min at room temperature and then sectioned at 35 μm thickness by using a vibratome. Sections were then processed for immunohistochemistry as described in ref. 23. Tissue sections were incubated free-floating with primary antibodies against

spinophilin (polyclonal IgG; 1:100; Upstate/Millipore), synaptophysin (monoclonal IgG; 1:2,000; Chemicon/Millipore), and/or HuC/D (monoclonal IgG; 1:100; Molecular Probes) at room temperature overnight. For a polyclonal antibody, tissue sections were incubated with Alexa Fluor 568 goat anti-rabbit IgG (1:200; Molecular Probes) for 3 h at room temperature. For monoclonal antibodies, sections were treated with a biotinylated secondary antibody (1:20; Vector Laboratories) for 3 h at room temperature and then with streptavidin conjugated with Alexa Fluor 488 (1:100; Molecular Probes) for 3 h at room temperature. Sections were mounted with VECTASHIELD mounting medium with DAPI to counterstain nuclei (Vector Laboratories) and imaged with the confocal microscope (512 pixels × 512 pixels).

All data were quantified by using the ImageJ program. The appearance of spinophilin and synaptophysin profiles in a 63-μm × 63-μm image, taken from the superficial part of the stratum radiatum, were analyzed with the photographic negative after background subtraction. The total number of spinophilin and synaptophysin granules were then counted by using ImageJ. Synaptophysin intensity was defined in the whole area of a 63-μm × 63-μm image. HuC/D immunostaining was quantified by measuring fluorescence intensity in the proximal dendrite portion of each individual CA1 pyramidal neuron. The naïve control data were set at 100%, and all other experiment data were defined as the percentage of their naïve control.

***In Vivo* EM.** At 1 day after the probe test (i.e., 2 days after water maze training), rats, anesthetized with choral hydrate, were perfused through the heart with PBS by gravity to wash out the blood and then fixed with ≈400 ml of 2% glutaraldehyde and 3% paraformaldehyde; removed brains were postfixed overnight with the same fixative at 4°C. Thereafter, hippocampi were isolated from the right brain hemispheres, and dorsal hippocampi were sectioned with a vibratome at 400 μm and then resectioned to 100 μm. Hippocampi were postfixed in 1% OsO_4. Electron micrographs (100 μm^2 CA1 area at ×5,000) were made of Epon-embedded hippocampal sections with a JEOL 200CX electron microscope. These sections were 90 nm thick and had been previously stained with uranyl acetate and lead citrate. During quantification, electron micrographs were digitally zoomed up to ×20,000 magnification by the default program Preview on an iMac G5 computer (Apple) with the Mac OS X operating system and a 19-inch monitor. Spines were defined as structures that formed synapses with axon boutons and did not contain mitochondria. Quantitative classification of dendritic spines as "mushroom" spines required that either (*i*) spine "heads" attached to a clearly distinguishable "neck" (e.g., Fig. 3*a*) have a cross-sectionally visualized diameter of >600 nm (8) as measured in ImageJ or (*ii*) spine "heads" not attached to a clearly distinguishable "neck" (e.g., Fig. 3*c*, Maze) have both (cross-sectionally visualized) long and short axis lengths of >600 nm. Increased numbers of presynaptic vesicles in axon boutons were measured as an increase in the frequency of axon boutons with presynaptic vesicles that occupied more than 50% cross-section space not occupied by other organelles.

Confocal *in Vitro* Experiments. Rats under halothane anesthesia were decapitated. Dorsal parts of hippocampi were then isolated and sectioned at 350 μm thickness at 4°C with a vibratome with ice-cold, artificial cerebrospinal fluid (aCSF) composed of 0 mM NaCl, 5 mM KCl, 2 mM $MgSO_4$, 2 mM $CaCl_2$, 26.2 mM $NaHCO_3$, 1.25 mM NaH_2PO_4, and 248 mM glucose (pH 7.4; 300 ± 10 mOsm). Hippocampal slices were recovered in aCSF [119 mM NaCl, 2.5 mM KCl, 1.3 mM $MgSO_4$, 2.5 mM $CaCl_2$, 26.2 mM $NaHCO_3$, 1 mM NaH_2PO_4, 11 mM glucose (pH 7.4; 300 ± 10 mOsm)] while bubbled with 95% O_2 and 5% CO_2 at 32°C. Hippocampal slices were then incubated in the incubator chamber with continuous perfusion of aCSF while being bubbled with 95% O_2 and 5% CO_2 at 32°C. At the end of the experiments, hippocampal slices were immersed in fixative composed of 4% paraformaldehyde in PBS for 30 min. After fixation, hippocampal slices were sectioned at 35 μm with a vibratome. Only sections deeper than 100 μm from the cut surface of hippocampal slices were used for immunohistochemistry of HuC/D and spinophilin and quantified as described above.

Statistical Analysis. All graphic data are shown as means ± SEM. All behavioral training and confocal data from confocal images were first statistically probed by ANOVA: single factor. Behavioral data with a significant overall difference among the groups as demonstrated with ANOVA were then further analyzed for between-group differences (e.g., maze vs. maze and bryostatin) with ANOVA: single factor. Confocal and EM data with a significant overall difference among the groups as demonstrated with ANOVA were further analyzed for between-group differences with paired two-tailed *t* test comparisons. All data were considered to show between-group significant differences at $P < 0.05$.

We thank Dr. S. Brian Andrews (Laboratory of Neurobiology, National Institute of Neurological Disorders and Stroke, National Institutes of Health) for valuable advice and discussions, and the National Institute of Neurological Disorders and Stroke Electron Microscopy and Light Imaging facilities for excellent technical assistance.

1. Cajal SR (1995) *History of the Nervous System of Man and Vertebrate* (Oxford Univ Press, New York).
2. Cajal SR (1991) *Histologie du Systeme Nerveux de l'Homme et des Vertebres* (Consejo Superior de Investigaciones Cientificas, Madrid).
3. Enger F, Bonhoeffer T (1999) *Nature* 399:66–70.
4. Matus A (2005) *Curr Opin Neurobiol* 15:67–72.
5. Matsuzaki M, Honkura N, Ellis-Davies GC, Kasai H (2004) *Nature* 429:761–766.
6. Matsuzaki M, Ellis-Davies GC, Nemoto T, Miyashita Y, Iino M, Kasai H (2001) *Nat Neurosci* 4:1086–1092.
7. Wilkinson SE, Parker PJ, Nixon JS (1993) *Biochem J* 294:335–337.
8. Harris KM, Jensen FE, Tsao B (1992) *J Neurosci* 12:2685–2705.
9. Geinisman Y, Berry RW, Disterhoft JF, Power JM, Van der Zee EA (2001) *J Neurosci* 21:5568–5573.
10. Quattrone A, Pascale A, Nogues X, Zhao W, Gusev P, Pacini A, Alkon DL (2001) *Proc Natl Acad Sci USA* 98:11668–11673.
11. Pascale A, Gusev PA, Amadio M, Dottorini T, Govoni S, Alkon DL, Quattrone A (2004) *Proc Natl Acad Sci USA* 101:1217–1222.
12. Pascale A, Amadio M, Scapagnini G, Lanni C, Racchi M, Provenzani A, Govoni S, Alkon DL, Quattrone A (2005) *Proc Natl Acad Sci USA* 102:12065–12070.
13. Bank B, Deweer A, Kuzirian AM, Ramussen H, Alkon DL (1988) *Proc Natl Acad Sci USA* 85:1988–1992.
14. Olds JL, Anderson ML, McPhie DL, Staten LD, Alkon DL (1989) *Science* 245:866–869.
15. LoTurco JJ, Coulter DA, Alkon DL (1988) *Proc Natl Acad Sci USA* 85:1672–1676.
16. Calabrese B, Halpain S (2005) *Neuron* 48:77–90.
17. Craske ML, Fivaz M, Batada NN, Meyer T (2005) *J Cell Biol* 170:1147–1158.
18. Matsuoka Y, Li X, Bennette V (1998) *J Cell Biol* 142:485–497.
19. Leuner B, Falduto J, Shors TJ (2003) *J Neurosci* 23:659–665.
20. Lamprecht R, Farb CR, Rodrigues SM, LeDoux JE (2006) *Nat Neurosci* 9:481–483.
21. Sun MK, Alkon DL (2002) *J Neurophysiol* 87:2441–2449.
22. Kirov SA, Petrak LJ, Harris KM (2004) *Neuroscience* 127:69–80.
23. Hongpaisan J, Winters CA, Andrews SB (2004) *J Neurosci* 24:10878–10887.
24. Etcheberrigaray R, Tan M, Dewachter I, Kuipéri C, Van der Auwera I, Wera S, Qiao L, Bank B, Nelson TJ, Kozikowski AP, *et al*. (2004) *Proc Natl Acad Sci USA* 101:11141–11146.